Available online at www.sciencedirect.com
SCIENCE DIRECT®
Bioorganic & Medicinal Chemistry 12 (2004) 6107–6118
Bioorganic & Medicinal Chemistry

Ionization, lipophilicity, and molecular modeling to investigate permeability and other biological properties of amlodipine

Giulia Caron,[a,*] Giuseppe Ermondi,[a] Alessandro Damiano,[a] Laura Novaroli,[a] Oksana Tsinman,[b] Jeffrey A. Ruell[b] and Alex Avdeef[b,†]

[a]*Dipartimento di Scienza e Tecnologia del Farmaco, Università di Torino, Via P. Giuria 9, I-10125 Torino, Italy*
[b]*pION Inc., 5 Constitution Way, Woburn, MA 01801, USA*

Received 30 March 2004; accepted 6 September 2004
Available online 29 September 2004

Abstract—This paper uses a recent approach toward drug discovery, in which in silico tools and experimental data are combined together to study the structural features of amlodipine and their relevance in the peculiar pharmacodynamic and pharmacokinetic profiles of this long acting calcium antagonist.

Results reveal for amlodipine two families of conformers (folded and extended) but also demonstrate that protonation is the predominant factor governing amlodipine intermolecular interactions among which ionic forces play a major role.

1. Introduction

1,4-Dihydropyridines (1,4-DHPs) are a well-known class of calcium antagonists, drugs used in the treatment of hypertension. The original lead compound of the class of 1,4-DHP is nifedipine, (**1** in Fig. 1) which is still widely used today in therapy. 1,4-DHPs can be classified either according to their pharmacodynamic properties and/or according to their pharmacokinetic properties (duration of action).[1–3] Amlodipine (**2** in Fig. 1), lacidipine (**3**), and lercanidipine (**4**) belong to the third generation of 1,4-DHPs, pharmacokinetically characterized by prolonged effect.[2,3]

Amlodipine (2-[(2-aminoethoxy)methyl]-4-(2-chlorophenyl)-3-ethoxycarbonyl-5-methoxycarbonyl-6-methyl-1,4-dihydropyridine)[4]) is comparable from a pharmacodynamic point of view (potency and selectivity) to

Abbreviations: 1,4-DHPs, 1,4-dihydropyridines; 1,2-dce, 1,2-dichloroethane/water system; AM1, Austin Model 1; ASA, the water-accessible surface area; ASA+, the positive surface area; $CASA^+$, the charge-weighted positive surface area; $FCASA^+$, the fractional charge-weighted positive surface area; HB, hydrogen bonding; HBD, H-bond donor acidity; HBA, H-bond donor basicity; GB/SA, generalized born surface area; HMC, Hybrid Monte Carlo; IAM, immobilized artificial membranes; $\log P^{N}_{oct}$, logarithm of the partition coefficient of the neutral form in the *n*-octanol/water; $\log P^{N}_{dce}$, logarithm of the partition coefficient of the neutral form in the 1,2-dichloroethane/water; $\log P^{N}_{dbe}$, logarithm of the partition coefficient of the neutral form in the *n*-dibutylether/water; $\log P^{N}_{lip}$, logarithm of the partition coefficient of the neutral form in the liposomes/water system; $\log D^{pH}_{oct}$, logarithm of the distribution coefficient at a given pH in the *n*-octanol/water system; $\log P^{I}_{oct}$, logarithm of the partition coefficient of an ionized species I in the *n*-octanol/water system; $\log P^{I}_{dce}$, logarithm of the partition coefficient of an ionized species I in the 1,2-dichloroethane/water system; *diff*$(\log P^{N-I})$, difference between the $\log P$ of the neutral form of a compounds and the $\log P$ of its ionized form; $\Delta\log P_{oct-dce}$, the difference of the partition coefficients of the neutral species in the *n*-octanol/water and 1,2-dichloroethane/water systems; $\log k^{IAM}_{w}$, logarithm of the IAM capacity factor; $\log k^{ODS}_{w}$, logarithm of the capacity factor extrapolated to 100% aqueous solvent in RP-HPLC (ODS column); PAMPA, parallel artificial membrane permeability assay; P_e (cm/s units), the effective permeability coefficient; UWL, unstirred water layers; P_m, the true membrane permeability; P_0, pH-independent intrinsic permeability; PC^+, the total positive partial charge; PEOE, partial equalization of orbital electronegativities; QSAR, quantitative structure–activity relationship; RMS, root mean square.

Keywords: Isotropic lipophilicity; Anisotropic lipophilicity; Permeability; PAMPA; Molecular dynamics simulation; ASA descriptors; Intramolecular effects.

† Contribution no. 10 from *p*ION in the series: *PAMPA—a Drug Absorption in vitro Model.* Ref. 14 is part 3 of the series.

* Corresponding author. Tel.: +39 011 6707282; fax: +39 011 6707687; e-mail: giulia.caron@unito.it

0968-0896/$ - see front matter © 2004 Elsevier Ltd. All rights reserved.
doi:10.1016/j.bmc.2004.09.004

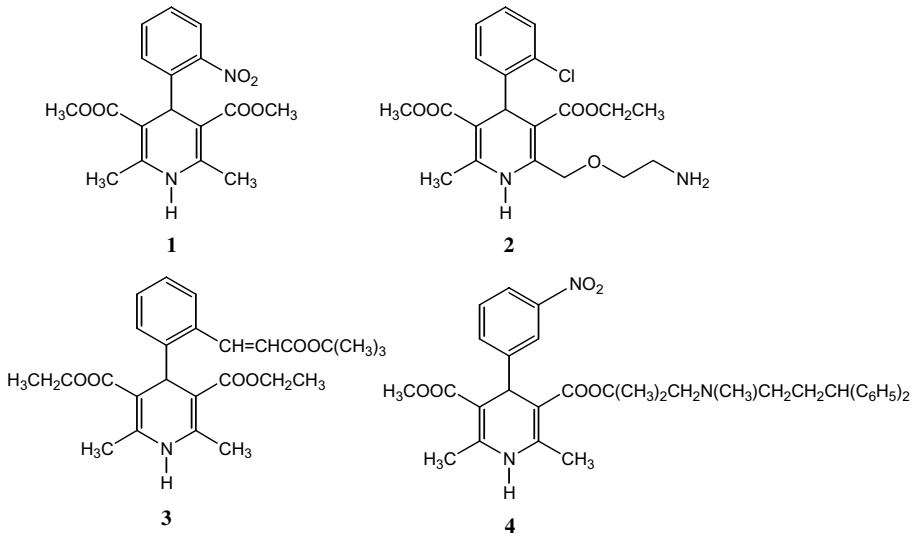

Figure 1. Chemical structures of nifedipine (**1**), amlodipine (**2**), lacidipine (**3**), and lercanidipine (**4**).

nifedipine, [5] but shows particularly favorable pharmacokinetic characteristics mainly due to the peculiar membrane location and binding mode,[6,7] which in turn are due to its structural features. Amlodipine in fact bears a basic 2-aminoethoxymethyl group on the DHP ring that is very different from substituents located in the same position on third generation 1,4-DHPs (Fig. 1) and strongly influences the ionization and lipophilicity profiles of the drug.

The deconvolution of information from ionization and lipophilicity data could furnish a simple prediction tool for membrane permeation ability useful in the design of long action drugs. In fact besides their numerical value lipophilicity data contain a variety of information about inter- and intramolecular forces affecting partitioning, binding, and their related biological phenomena.[8–11] In this paper a sort of 'in combo' approach[12] has been undertaken to extract structural information related to pharmacokinetic properties from ionization and lipophilicity results. In particular the strategy consists of three steps: (a) measurement, collection, and analysis of experimental data concerning ionization and lipophilicity in various systems; (b) simple and reliable in vitro permeability measurements,[13,14] and (c) molecular modeling investigations. For the sake of completeness, nifedipine was used as reference compound.

2. Results and discussion

2.1. Ionization behavior

For **2** experimental values of pK_a can be divided in two groups: (a) direct aqueous values (9.07 here, 9.02 in Ref. 6, 9.26 in Ref. 15) and (b) extrapolated aqueous values (9.03 in Ref. 16 using methanol as co-solvent, 9.31 in Ref. 17 using dioxane as co-solvent). All measurements are in good agreement (differences less than 0.5). In this study an averaged value of 9.1 was used.

The experimental pK_a value is sufficiently well predicted by both SPARC[18] (8.6) and ADME Boxes[19] (9.6). Because of the good agreement between experimental and calculated values no particular intramolecular interaction is expected to occur in water neither for the neutral nor the ionized species.

2.2. Lipophilicity behavior

2.2.1. Lipophilicity in isotropic systems. Information arising from isotropic lipophilicity (water/solvent system in which the lipophilic phase is an organic solvent) is less bio-mimetic than lipophilicity in anisotropic media (e.g., liposomes), but a number of reports recently stressed how much information is hidden in log$P$ data.[8,20–22]

2.2.1.1. Neutral species. Isotropic lipophilicity of neutral amlodipine was firstly investigated in *n*-octanol/water system.

Experimental potentiometric values for amlodipine are reported in Ref. 16 ($\log P^{N}_{oct} = 2.96$) and in Ref. 17 ($\log P^{N}_{oct} = 3.17$) and are in good agreement. The experimental value for nifedipine is more doubtful but among data reported in MedChem95 databases the values of Mason (2.86) and Manners (3.27) were selected because the same authors reported a number of reliable lipophilicity data for amlodipine. In addition, Lombardo et al.[23] reports 3.17 for **1**. We assumed for nifedipine an averaged log$P$ = 3.0. It should be pointed out that nifedipine log$P$ cannot be determined by potentiometry and is almost experimentally inaccessible by traditional shake-flask method, which reasonably has log$P$ = 3.0 as upper limit of detection.[8]

Calculated values of lipophilicity have been obtained by testing various log$P$ software programs based on different methodologies.[22] For amlodipine and nifedipine calculated data variances have been illustrated by a histogram and compared with experimental $\log P^{N}_{oct}$

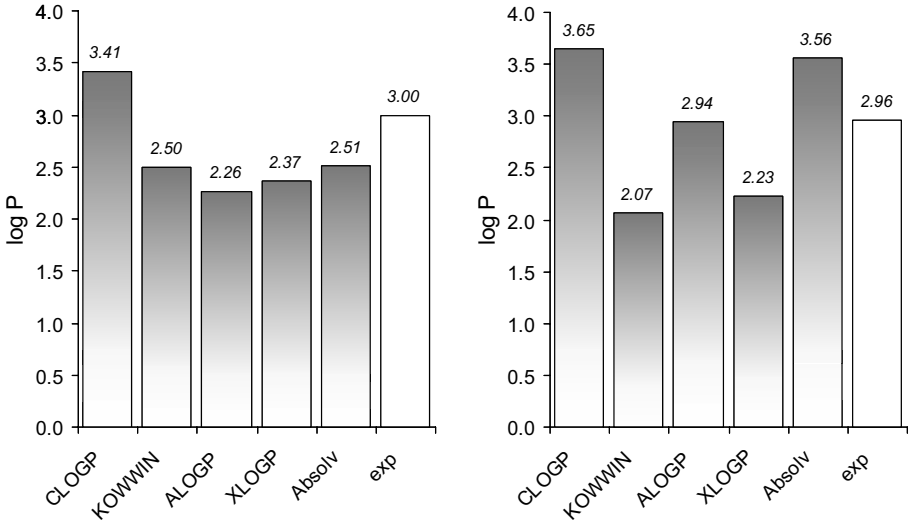

Figure 2. Comparison between calculated $\log P^{N}_{oct}$ and selected experimental values: nifedipine on the left and amlodipine on the right. For further details see text.

(Fig. 2): the sufficient agreement between calculated data and experimental results suggests that no intramolecular effects govern lipophilicity of neutral amlodipine (and nifedipine) in the octanol/water system. In particular we chose Absolv[24] as reference software for calculating $\log P$ (Table 1) because it is able to calculate $\log P^{N}$ in various biphasic systems.[22]

Table 1. Isotropic lipophilicity descriptors for neutral amlodipine and nifedipine

Descriptor	Amlodipine	Source	Nifedipine	Source
$\log P^{N}_{oct}$ [a]	2.96	Ref. 16	3.0	Med-Chem95
$\mathrm{clog}P^{N}_{oct}$ [b]	3.56	Absolv	2.51	Absolv
diff$(\log P^{exp-calc})$ [c]	−0.60	Here	0.49	Here
$\log P^{N}_{dce}$ [d]	4.02	Here	>3	—
$\mathrm{clog}P^{N}_{dce}$ [e]	2.89	Absolv	3.23	Absolv
diff$(\log P^{exp-calc})$ [f]	1.13	Here	—	—
$\Delta\log P_{oct-dce}$ [g]	−1.06	Here	—	—
$c\Delta\log P_{oct-dce}$ [h]	0.88	Ref. 27	0	Ref. 27
$\log P^{N}_{dbe}$ [i]	1.52	Here	—	—
$\mathrm{clog}P^{N}_{dbe}$ [j]	2.06	Absolv	1.32	Absolv
diff$(\log P^{exp-calc})$ [k]	−0.54	Here	—	—

[a] Experimental value of the logarithm of the partition coefficient of the neutral form in *n*-octanol/water system.
[b] Calculated value (Absolv) of the logarithm of the partition coefficient of the neutral form in *n*-octanol/water system.
[c] Difference between footnotes a and b.
[d] Experimental value of the logarithm of the partition coefficient of the neutral form in 1,2-dce/water system.
[e] Calculated value (Absolv) of the logarithm of the partition coefficient of the neutral form in 1,2-dce/water system.
[f] Difference between footnotes d and e.
[g] Difference between footnotes a and d.
[h] See text and cited reference for details.
[i] Experimental value of the logarithm of the partition coefficient of the neutral form in the *n*-dibutylether/water system.
[j] Calculated value of the logarithm of the partition coefficient of the neutral form in the *n*-dibutylether/water system.
[k] Difference between footnotes i and j.

The 1,2-dichloroethane/water (1,2-dce) was selected as the second solvent system to investigate isotropic lipophilicity of **1** and **2** because 1,2-dce shows different polar properties compared to *n*-octanol and thus enables intramolecular effects to be investigated.[22,25]

The experimental $\log P^{N}_{dce}$ value is 4.02 for **2** (Table 1), whereas Absolv predicts 2.89. In this case the experimental lipophilicity of amlodipine is much higher than expected. Indeed Absolv predicts well both $\log P^{N}_{oct}$ and $\log P^{N}_{dbe}$ ($\log P^{N}$ in the *n*-dibutylether/water, see below) for **2** and also $\log P_{oct}$ for nifedipine. Thus, the difference found in the 1,2-dce/water between experiments and theory seems to be due to intramolecular effects affecting neutral amlodipine in apolar solvents.

This intramolecular effect has been demonstrated by another approach: the analysis of the difference of partition coefficients in *n*-octanol/water and 1,2-dichloroethane/water ($\Delta\log P_{oct-dce}$) by a graphical tool.[8,26] To a first approximation, for neutral species, $\Delta\log P_{oct-dce}$ is rather constant for compounds with similar H-bond donor acidity (HBD) and H-bond donor basicity (HBA) properties. In this case, the average $\Delta\log P_{oct-dce}$ represents the value of the *y*-intercept of the plot experimental $\log P_{oct}$ versus experimental $\log P_{dce}$ (see Fig. 3). HBD properties (defined as the number of polar atoms able to donate one or more hydrogen atoms to form a HB) split the set of reference compounds[26,27] in three categories. Thus, an anomalous value of $\Delta\log P_{oct-dce}$ corresponds to an outlier in Figure 3, suggesting specific intramolecular interactions affecting the lipophilicity either in octanol/water or in 1,2-dce/water. Amlodipine (HBD = 2) is an outlier because the true location on the graph is different from expected location: in fact **2** falls on the regression lines obtained for pure H-bond acceptors solutes despite its HB donor characteristics. The location of amlodipine in the plot is due to an anomalous value $\log P^{N}_{dce}$, being $\log P^{N}_{oct}$ in the predictable range (see above).

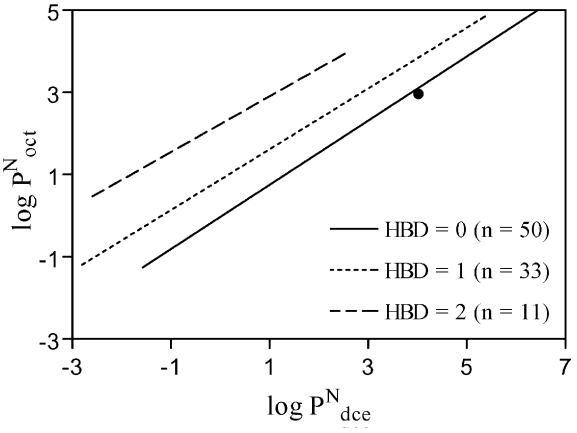

Figure 3. The graphical representation of experimental $\log P^{N}_{oct}$ versus $\log P^{N}_{dce}$: a tool to investigate the HB properties (mainly HBD) of compounds. The position of amlodipine is indicated by a dot.

Taken together, these data suggest that the H-bonding donor character of neutral amlodipine cannot be expressed fully in 1,2-dichloroethane/water system, probably because of the formation of intramolecular interactions whose chemical nature will be investigated in details below by conformational analysis.

Finally, the lipophilicity of amlodipine in *n*-dibutylether/water (Table 1) turns out to be as the expected lipophilicity in the standard *n*-octanol/water system;[28] for chloroform/water the paucity of available data does not allow a full interpretation of results (data for amlodipine not reported).

2.2.1.2. Cationic species. Also for cationic amlodipine, isotropic lipophilicity was firstly investigated in the *n*-octanol/water system. Experimental potentiometric $\log P^{I}_{oct}$ is 1.15 (Table 2). This value is larger than expected. In fact, by assuming a difference of about three log units (*diff*$(\log P^{N-I})$[8]) between lipophilicities of neutral and ionized species, $\log P^{I}$ is expected to be about 0.

In 1,2-dce/water system we measured $\log P^{I} = -0.78$. This value is in line with a *diff*$(\log P^{N-I})$ of about 5 as commonly found in this solvent system.[29] However, the *diff*$(\log P^{N-I})$ is only apparently normal. In fact we have already demonstrated (see above) that the lipophilicity of neutral amlodipine is influenced by intramolecular effects and thus to have a normal *diff*$(\log P^{N-I})$ it is necessary to admit that also cationic amlodipine is affected by intramolecular effects.[8] Conformational analysis (see below) confirms this hypothesis.

For *n*-dibutylether/water solvent systems, not enough information is available to discuss experimental data reported in Table 2.

2.2.2. Lipophilicity in anisotropic biphasic systems (non-chromatographic methods). In Ref. 30, anisotropic biphasic systems have been defined as systems in which the lipophilic phase is a suspension of micelles or liposomes. Anisotropic lipophilicity descriptors for amlodipine and nifedipine are listed in Table 3.

Table 2. Isotropic lipophilicity descriptors for cationic amlodipine

Descriptor	Amlodipine	Source
$\log D^{7.4\,a}_{oct}$	1.55	Ref. 16
$\log P^{I\ b}_{oct}$	1.15	Ref. 16
$\mathrm{clog}P^{I\ c}_{oct}$	−0.04	$\log P^{N-3}_{oct}$
diff$(\log P^{N-I})^{d}$	1.81	Here
$\log D^{7.4\,e}_{dce}$	2.40	Here
$\log P^{I\ f}_{dce}$	−0.78	Here
$\mathrm{clog}P^{I\ g}_{dce}$	−0.98	$\log P^{N-5}_{dce}$
diff$(\log P^{N-I})^{h}$	4.80	Here
$\log D^{7.4\,i}_{dbe}$	−0.08	Here
$\log P^{I\ j}_{dbe}$	−2.23	Here
$\mathrm{clog}P^{I\ k}_{dbe}$	−1.98	$\log P^{N-3.5}_{dbe}$
diff$(\log P^{N-I})^{l}$	3.75	Here

[a] Logarithm of the distribution coefficient at pH 7.4 in *n*-octanol/water experimentally determined.
[b] Experimental value of the logarithm of the partition coefficient of the ionized species in *n*-octanol/water system.
[c] Calculated value (details in the text) of the logarithm of the partition coefficient of the ionized species in *n*-octanol/water system.
[d] $\log P^{N} - \log P^{I}$ in *n*-octanol/water system.
[e] Logarithm of the distribution coefficient at pH 7.4 in 1,2-dce/water experimentally determined.
[f] Experimental value of the logarithm of the partition coefficient of the ionized species in 1,2-dce/water system.
[g] Calculated value (details in the text) of the logarithm of the partition coefficient of the ionized species in 1,2-dce/water system.
[h] $\log P^{N} - \log P^{I}$ in 1,2-dce/water system.
[i] Logarithm of the distribution coefficient at pH 7.4 in *n*-dibutylether/water experimentally determined.
[j] Experimental value of the logarithm of the partition coefficient of the ionized species in *n*-dibutylether/water system.
[k] Calculated value (details in the text) of the logarithm of the partition coefficient of the ionized species in *n*-dibutylether/water system.
[l] $\log P^{N} - \log P^{I}$ in *n*-dibutylether/water system.

The anisotropic lipophilicity of nifedipine is 3.0.[3] The corresponding value for amlodipine is higher (4.30, Table 3). This means that, for **2**, $\log P^{N}_{lip}$ is greater than $\log P^{N}_{oct}$; but the two values are equal for **1**.

In liposomes/water, cationic amlodipine is as lipophilic as its neutral form. This behavior has been also observed for 4-phenylbutylamine[7] (a compound bearing a terminal primary amine but unable to form intramolecular hydrogen bonds), which seems to indicate that a very low *diff*$(\log P^{N-I})_{lip}$ (0.0 for amlodipine and 0.3 for 4-phenylbutylamine, Table 3) is a characteristic of primary amines.

These data have been already rationalized[6,7,31–33] by postulating that the charged amino portion of amlodipine interacts with the anionic oxygen of the phospholipid head group of the membrane bilayer, leading to an additional stabilization not possible for nifedipine. In addition, a specific mechanism of interaction (due the presence of H-bonds between the N–H groups of the neutral form and the phosphate groups) is present, not only for charged amlodipine but also for the neutral species.

2.2.3. Chromatographic indices (including IAM). RP-HPLC and IAM chromatographic indices for 1,4-DHPs have been reported in Refs. 34 and 35. Because of the

Table 3. Chromatographic data, anisotropic lipophilicity descriptors, and PAMPA permeability values for amlodipine and nifedipine

Descriptor[a]	Amlodipine	Source	Nifedipine	Source
Elog D (pH = 7.4)	2.15	Ref. 35	2.84	Ref. 35
log $k'w$ (pH = 7.4)	1.72	Ref. 35	2.34	Ref. 35
log k_w^{ODS} (pH = 7.0)	1.33	Ref. 34	2.45	Ref. 34
log k_w^{IAM} (pH = 7.0)	2.59	Ref. 34	1.74	Ref. 34
log P_{lip}^{N}	3.75	Ref. 7	—	—
log P_{lip}^{+}	3.75	Ref. 7	—	—
log K_p (pH = 7.0)[b]	4.30	Ref. 3	3.0	Ref. 3
log P_e (pH = 5.2)[c]	−3.52	Here	ei[g]	—
%R (pH = 5.2)[d]	88	Here	ei[g]	—
log P_e (pH = 6.4)[c]	−2.99	Here	ei[g]	—
%R (pH = 6.4)[d]	89	Here	ei[g]	—
log P_e (pH = 7.6)[c]	−2.99	Here	ei[g]	—
%R (pH = 7.6)[d]	89	Here	ei[g]	—
log P_e (pH = 8.8)[c]	−2.86	Here	ei[g]	—
%R (pH = 8.8)[d]	89	Here	ei[g]	—
log P_e (pH = 10.0)[c]	−2.86	Here	ei[g]	—
%R (pH = 10.0)[d]	89	Here	ei[g]	—
log P_0[e]	0.45	Here	ei[g]	—
log P_u[f]	−2.87	Here	ei[g]	—

[a] Descriptors details are reported in the original references.
[b] The definition reported by the authors mentions K_p as the membrane partition coefficient but it is clearly a distribution coefficient.
[c] Logarithm of P_e (the effective membrane permeability) at indicated pH.
[d] Percentile of compound retained by the filter-immobilized artificial membranes at indicated pH.
[e] Logarithm of P_0 (the permeability of the neutral form of amlodipine).
[f] Logarithm of P_u (the unstirred water layer (UWL) permeability.
[g] Experimentally inaccessible (see text for explanations).

pH used (ranging from 7 to 7.4) these indexes refer to cationic amlodipine.

RP-HPLC log k_w^{ODS} (logarithm of the capacity factor extrapolated to 100% aqueous solvent in RP-HPLC) values for **2** are always lower than those of **1**; for the series of nine 1,4-DHPs studied in Ref. 34, the plot log $D_{oct}^{7.4}$ versus log k_w^{ODS} shows a straight line (r^2 = 0.94), in which amlodipine is not detected as an outlier. Chromatographic indexes obtained using polar solvents thus indicate a normal behavior for cationic amlodipine.

When log k_w^{IAM} replaces log k_w^{ODS}[34] amlodipine is a strong outlier in the plot log $D_{oct}^{7.4}$ versus log k_w^{IAM}. This finding confirms that IAM indices are good descriptors of the strong interactions of basic amlodipine with membranes mainly due to the presence of the protonated amino group.

2.3. Molecular modeling

The complete deconvolution of information from ionization and lipophilicity data to be employed in pharmacokinetic prediction requires computational tools. In this study we used conformational analysis to investigate the molecular flexibility of amlodipine and the ASA (accessible surface area) descriptors to check the relevance of protonation in the 3D structure.

2.3.1. Molecular dynamics simulations. X-ray crystallographic investigation of an amlodipine analog[4] and of the maleate salt[6] indicates the existence of an intramolecular HB between the hydrogen linked to the nitrogen of the dihydropyridine ring and the ether oxygen of the basic chain.

Conformational analysis has been performed (see Section 4) to identify the most stable geometries under various conditions and thus the presence of intramolecular HB. Calculations have been performed on both enantiomers of amlodipine but giving similar results; below we refer to the *S* enantiomer.

Besides the expected 1,4-DHP structural features,[36] for amlodipine the formation of three intramolecular hydrogen bonds (HB) is possible (a) between the hydrogen linked to the nitrogen of the 1,4-dihydropyridine ring and the ether oxygen of the basic chain; (b) between the ether oxygen of the basic chain and the hydrogens linked to the basic primary amine, and (c) between hydrogens linked to the basic primary amine and the ester carbonyl (ether) oxygen of the lateral chain in 3 of the 1,4-DHP ring.

2.3.1.1. In vacuo results. For neutral amlodipine, 22 conformers have been found covering an energy range of about 46 kcal/mol and eight conformers differ from less than 10 kcal/mol from the most stable (conformer nev2 in Fig. 4A). The nine most stable conformers (within the 10 kcal/mol) do not show any intramolecular HB except for conformer nev10 (Fig. 4C), which has two intramolecular HBs. AM1 minimization performed on the most stable conformer (Fig. 4B) showed that semiempirical conditions increase planarity. Interestingly, according to AM1 calculations conformer nev10 (Fig. 4D) is more or less as stable as conformer nev2 (Fig. 4B) and thus nev10 can be responsible for higher than expected log P_{dce}^{N} value.

Also for cationic species 22 conformers have been found, covering an energy range of about 46 kcal/mol and 12 conformers differ from less than 10 kcal/mol from the most stable cav201 (Fig. 5A); a second conformer is found differing from the first one from less than 1 kcal/mol. All 13 conformers show at least an intramolecular HB: the five most stable form an HB between hydrogens linked to the basic primary amine and the ester carbonyl oxygens, the others are consistent with the X-ray data. AM1 minimization performed in vacuo on the most stable conformer (Fig. 5B) confirms the presence of the intramolecular HB which can be responsible for higher than expected log P_{dce}^{I} value.

2.3.1.2. The effect of solvation. For neutral species, 23 conformers have been found covering an energy range of 107 kcal/mol, with the two most stable conformers close in energy and completely extended (no intramolecular HB is formed). AM1 minimization (water conditions) confirms these findings.

For cationic species, 22 conformers have been found, covering an energy range of 90 kcal/mol, but only three

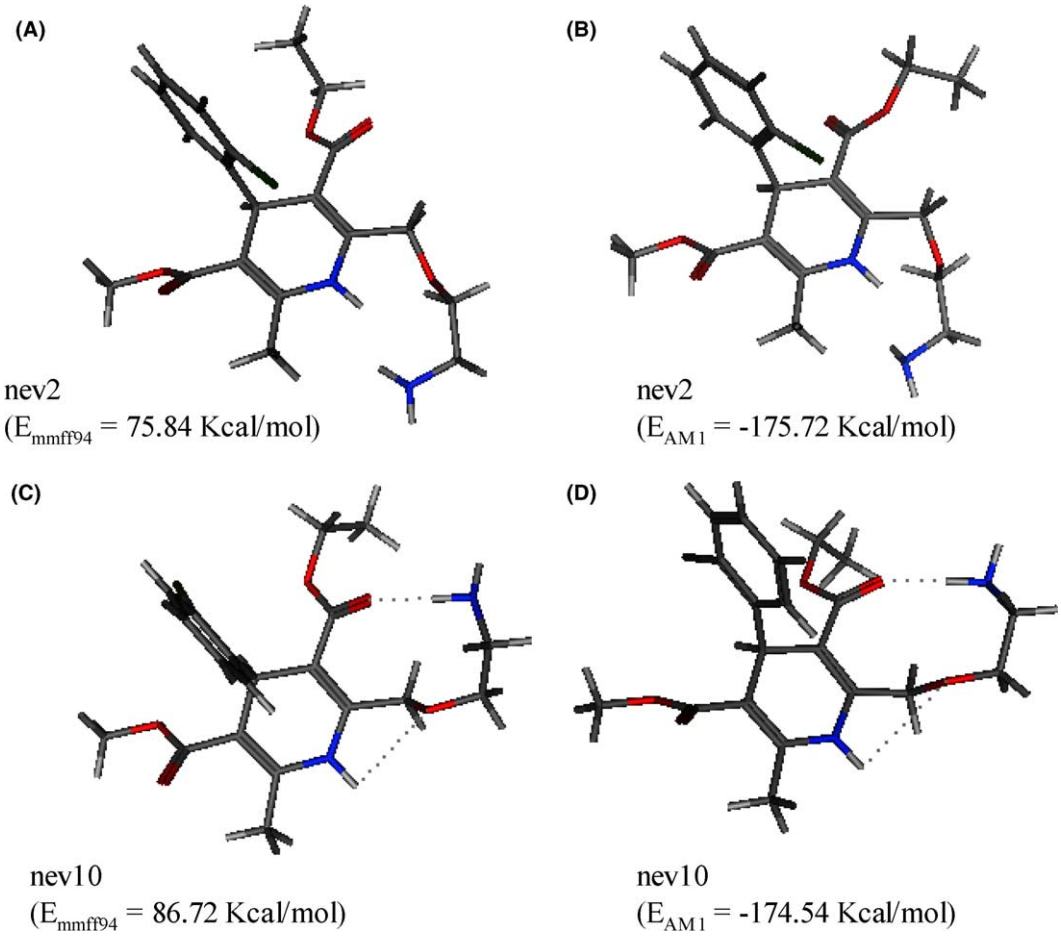

Figure 4. Conformation analysis results for neutral amlodipine in vacuo. (A) The most stable conformer (nev2) obtained by the conformational analysis, (B) the most stable conformer (nev2) obtained by the conformational analysis and minimized by AM1, (C) the most stable conformer (nev10) with intramolecular HB (shown in dots) obtained by the conformational analysis, and (D) the most stable conformer (nev10) with intramolecular HB (shown in dots) obtained by the conformational analysis and minimized by AM1.

of them are close in energy with the most stable, cas204 (Fig. 5C). Intramolecular HB occurs between the hydrogen linked to the nitrogen of the 1,4-dihydropyridine ring and the ether oxygen of the basic chain and affects only the two most stable geometries. AM1 calculation performed on the most stable conformers indicates the low stability of the intramolecular HB which is lost in all cases (shown in Fig. 5D for cas204).

Conformational analysis of amlodipine was already undertaken in Ref. 37, but the presence of intramolecular HB has not been investigated. Nevertheless data reported in Ref. 37 are in good agreement with our analysis (except for the neutral species in vacuo), indicating different conformational preferences for neutral and ionized species. In addition, this different behavior is also governed by the polar/apolar nature of the medium which, if polar, weakens the intramolecular electrostatic interactions that stabilize the folded conformers.

2.3.2. ASA descriptors. Calculated molecular properties from 3D molecular fields are a valuable approach to correlate 3D molecular properties with physicochemical, pharmacokinetic, and pharmacodynamic properties.[38] Unfortunately, many molecular fields[39,40] have severe limitations to handle charged species and thus are unable to investigate the feature of the positive charge born by **2** at physiological pH which is responsible for the ionic interactions that are mainly responsible for the high lipophilicity found for cationic amlodipine.

Thus to check the relevance of protonation for amlodipine (i.e., how similar are the cationic folded conformers to the neutral species), $FCASA^+$ descriptors (see Section 4 for definition) have been used. These latter belong to the accessible surface area (ASA)[41,42] descriptors which combine molecular surface area and partial atomic charges, and thus not only depend on the partial charges of the molecules but also on their conformations.

To check the relevance of drug flexibility to molecular properties, $FCASA^+$ were calculated (Table 4) for all conformers arising from conformational analysis with solvation conditions of amlodipine (neutral and cationic) and phenylbutylamine (neutral and cationic). The $FCASA^+$ range (the difference between the highest and the lowest value) is significantly larger for cationic amlodipine (0.31) than for cationic phenylbutylamine (0.05). Even if less evidently the same result is also found for neutral species (0.20 for amlodipine and 0.05 for

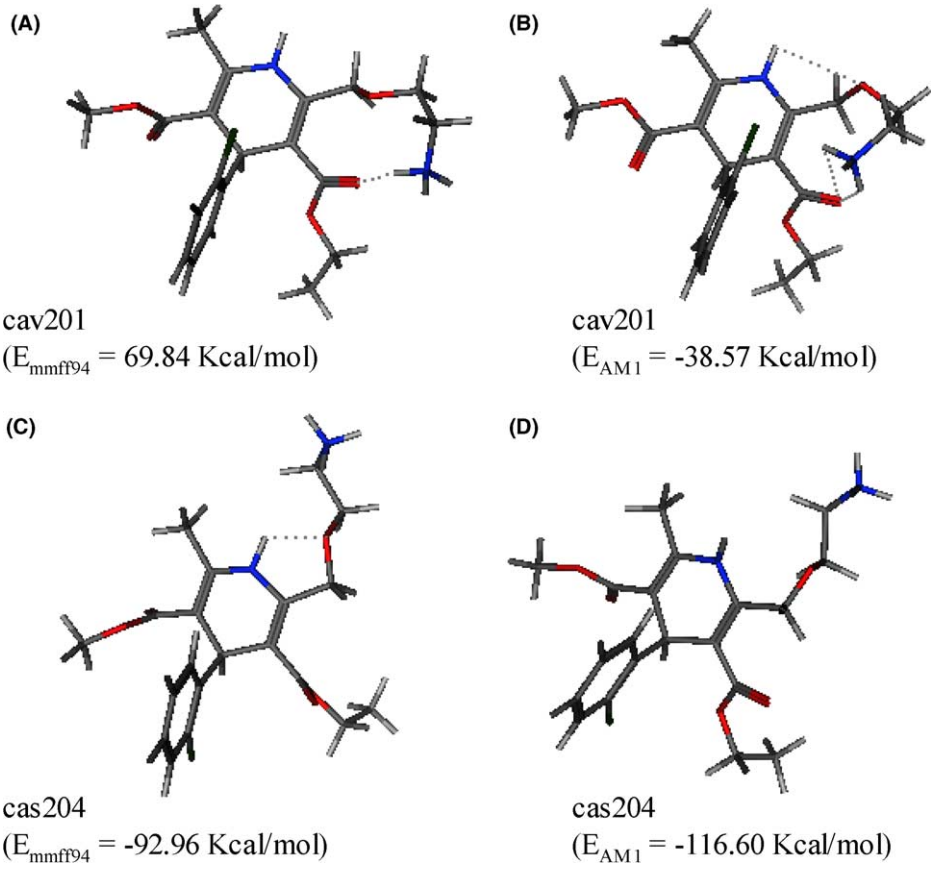

Figure 5. Conformation analysis results for cationic amlodipine. (A) The most stable conformer (cav201) obtained by the conformational analysis in vacuo, (B) the most stable conformer (cav201) obtained by the conformational analysis and minimized by AM1 in vacuo, (C) the most stable conformer (cas204) obtained by the conformational analysis in water (see Section 4 for details), and (D) the most stable conformer (cas204) obtained by the conformational analysis and minimized by AM1 in water (see Section 4 for details).

Table 4. ASA descriptors for neutral and cationic amlodipine and for neutral and cationic phenylbutylamine (PBA)

Descriptor	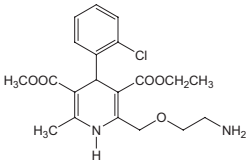	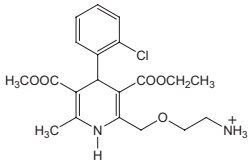	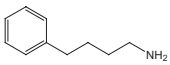	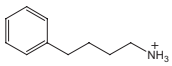
$FCASA^{+}_{low}$	1.66	2.41	0.52	1.29
$FCASA^{+}_{high}$	1.86	2.72	0.57	1.36
Range	0.20	0.31	0.05	0.05

phenylbutylamine). These findings confirm that amlodipine conformers are very different from one another.

As expected, the $FCASA^{+}$ range for neutral phenylbutylamine (0.52–0.57) is not superimposable onto the corresponding range (1.29–1.36) of its cationic species. Interestingly the same finding is shown for amlodipine, and clearly indicates that for amlodipine the charge is exposed on the molecular surface and also in folded conformers, and thus it is able to generate ionic interactions. This is probably a general feature for primary amines; further studies are in due course in our laboratory to give more insight in this topic.

2.4. Permeability data

The recently developed in vitro drug absorption model, called parallel artificial membrane permeability assay (PAMPA), first described by Kansy et al.[43] was used to measure membrane permeability coefficients of amlodipine. The effective permeability coefficient, P_e (cm/s units), determined by the method, is a measure of the rate constant which characterizes the passive-diffusion transport of a molecule across a barrier formed from the artificial phospholipid membrane and the two unstirred water layers (UWL) adjacent to each side of the membrane.

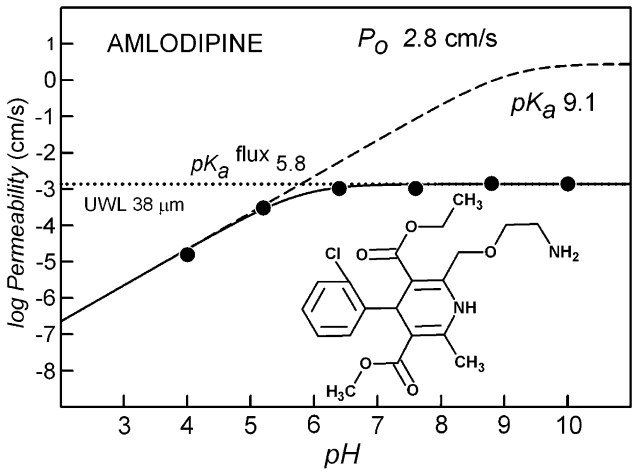

Figure 6. Gradient-pH mapping PAMPA for amlodipine.

For ionizable molecules (is not possible to apply the same technique to extract the intrinsic permeability of nifedipine), the plot of $\log P_e$ versus pH is hyperbolic in shape (Fig. 6), with the diagonal (slope +1 for bases and −1 for acids) and horizontal (slope 0) curve tangents intersecting at a pH called the *flux* pK_a (pK_a^{flux}).[13] This unique pH value defines the point where the resistance to transport is 50% due to the UWL and 50% due to the artificial membrane barrier. For lipophilic molecules, such as amlodipine, the UWL is rate limiting in transport, and the highest measured $\log P_e$ values correspond approximately to the UWL permeability. The true permeability is hidden, but can be calculated in the assay if the true pK_a of the molecule is known. After the elimination of the effect of the UWL, the resulting curve, $\log P_m$ versus pH, represents the true permeability. The highest position in the curve (2.8 ± 0.5 cm/s for amlodipine, Fig. 6), indicates $\log P_0$, which corresponds to the intrinsic permeability coefficient of the molecule. (By analogy to octanol–water partition experiments, the $\log P_m$ versus pH curve is like the $\log D_{oct}$ versus pH curve, and $\log P_0$ is like $\log P_{oct}^N$).

The results (Table 3) indicate that neutral amlodipine ($\log P_0 = 0.62$) is highly permeable as also confirmed by calculations (ADME Boxes, Ref. 19) and in agreement with the finding that after oral administration, amlodipine is almost completely absorbed;[44] conversely, cationic amlodipine does not permeate across artificial phospholipid barriers, this latter highly discriminating against charged species.

In the literature a linear dependence of permeability from $\log P_{alk}$ has been shown.[45] Our results confirm this finding. In fact, the highly permeable neutral amlodipine shows high $\log P_{dce}^N$ (higher than expected, see above), whereas 1,2-dce/water expresses about the same intermolecular forces than alkane/water system.[26] Conversely, cationic amlodipine does not permeate and is highly retained in the PAMPA system probably because of the strong ionic interactions with phospholipids already evidenced by the partitioning behavior in liposomes/water system.

2.5. The pharmacodynamic and pharmacokinetic relevance of lipophilicity, permeability, and molecular modeling data

The combined analysis of $\log P$ data and molecular modeling results reveals for amlodipine two families of conformers (folded and extended) whose reciprocal predominance varies with (a) the electrical state of the drug (neutral/ionized) and (b) the polar and/or anisotropic characteristics of the medium. Indeed ASA descriptors also demonstrate that protonation and not conformational variability is the predominant factor governing amlodipine intermolecular interactions and, among the latter, ionic forces play a major role.

From a pharmacodynamic point of view, ionic interactions are of poor significance. In fact the introduction of a basically substituted alkyl chain linked to the DHP 2-methyl group via an ether oxygen atom does not significantly lower potency and vascular selectivity of **2** compared to **1**.[4] Additional QSAR studies[46] also demonstrated that the basic center was not an absolute requirement for calcium antagonist activity and that the amino function could be replaced by polar heterocycles. Interestingly these last structures lost the pharmacokinetic optimal profile exhibited by amlodipine.

Ionic interactions play a fundamental role in determining pharmacokinetics of amlodipine because they are responsible for the long stay in membrane which in turn is mandatory for the large volume of distribution, V_d, (25 L/kg[4]) and the long plasma half life (30 h in Ref. 4). The extent of ionization and the balance between ionic and hydrophobic interactions are, therefore, the crucial features which differentiate the membrane binding mode of amlodipine from other long acting calcium antagonists (e.g., lacidipine and lercanidipine).[42]

3. Conclusion

The peculiar interactions of amlodipine with biological membranes have been generally demonstrated and studied in recent years by using biphasic anisotropic systems; conversely, the full characterization of its physicochemical profile had not been undertaken. In this paper a strategy of combining isotropic and anisotropic lipophilicity, permeability, and molecular modeling tools was adopted to study the structural features of amlodipine and their relevance in rationalizing its pharmacological profile.

Taken together lipophilicity showed anomalously high values for cationic amlodipine in all systems, while neutral species appear more lipophilic than expected only in an apolar solvent such as 1,2-dce.

The correspondence between molecular dynamics simulation and partitioning results was used to explain experimental results. In fact simulations in vacuo mimic partitioning systems in which the organic phase is apolar

(e.g., 1,2-dce) while aqueous simulation give a representation of systems for which the organic phase is more similar to water as in the case of *n*-octanol.

The protonation of the substituted ethanolamine moiety undoubtedly governs molecular properties of amlodipine and its biological behavior. This moiety is widely used in drug design to enhance solubility and bioavailability of potential drug candidates with poor pharmacokinetic profile. Work is in progress to extend this study to a number of potential drug candidates bearing substituted ethanolamine moiety in the effort of extracting more general rules of wider application.

4. Experimental

4.1. Material

Amlodipine was extracted from Novasc® (Pfizer). Nifedipine was purchased from Sigma (Milan, Italy).

PAMPA phospholipid was obtained from *p*ION (GIT-0, Double-Sink™ lipid, PN 110669), and was stored at −20 °C when not used. Spectroscopic grade dimethylsulfoxide was purchased from Burdick & Jackson (Muskegon, MI, USA). The pH of the assayed solutions was adjusted with a universal buffer (*p*ION, PN 100621), and a buffer solution at pH 7.4 containing a chemical scavenger to simulate serum proteins (*p*ION, ASB-7.4 Double-Sink™ buffer, PN 110139).

4.2. Ionization and lipophilicity

Aqueous pK_a values were determined for amlodipine by a pH-metric technique using a GLpKa apparatus[11] (Sirius Analytical Instruments Ltd, Forrest Row, East Sussex, UK) as described in detail elsewhere.[11]

To gain more insights into the structural features of amlodipine apparent ionization constants (p$_s K_a$) have been obtained by potentiometry in methanol mixtures because of the low aqueous solubility of compounds.[47] Aqueous pK_a values have been obtained by extrapolation using the Yasuda–Shedlovsky (YS) procedure.[48]

Experimental log P^N, log P^I, and log $D^{7.4}$ values were obtained by pH-metric technique using a GLpKa apparatus[11] (Sirius Analytical Instruments Ltd, Forrest Row, East Sussex, UK) as described in detail elsewhere[11] by using various organic solvents.

To validate log P^I shake-flask experiments have been traditionally performed.[9] Ionic strength was adjusted to be 0.15 M in KCl.

4.3. Parallel artificial membrane permeability assay (PAMPA)

4.3.1. PAMPA method. The PAMPA Evolution instrument from *p*ION INC (Woburn, MA, USA) was used in this study.

In PAMPA, a 'sandwich' is formed from a 96-well microtitre plate (*p*ION, PN 100611) and a 96-well filter plate (Millipore, IPVH brand), such that each composite well is divided into two chambers: donor at the bottom and acceptor at the top, separated by a 125 μm microfilter disc (0.45 μm pores), coated with a 20% (wt/v) dodecane solution of a lecithin mixture (*p*ION GIT-0, PN 110669). This phospholipid is more concentrated than used previously.[13,21,43,49–57]

The effective permeability, P_e, was measured from pH 4.0 to 10.0, using five to six approximately equally spaced pH values to ensure obtaining values above and below the apparent pK_a value (pK_a^{flux}) of the compounds.

Drug samples were introduced as 10 mM DMSO stock solutions in a 96-well polypropylene microtitre plate. The robotic liquid handling system draws a 3–10 μL aliquot of the DMSO stock solution and mixes it into an aqueous buffer solution, so that the final typical sample concentration is 10–50 μM and the DMSO concentration is <1% (v/v).

The drug solutions were filtered using a 96-well filter plate (Corning, PVDF), and added to the donor compartments. The donor solutions were varied in pH (NaOH-treated universal buffer, *p*ION, PN 100621), while the acceptor solution had the same pH 7.4 (*p*ION, PN 110139). Each donor well employed a magnetic stirrer, with speed set to produce about a 30–40 μm unstirred water layer, to mimic the thickness of the layer found in the intestine.[58]

The sandwich was formed and allowed to incubate for no longer than 30 min (15 h was the original permeation time used by Kansy and co-workers), in a sealed box (*p*ION Gut-Box™) containing constant humidity and an oxygen and a carbon dioxide scrubber. The sandwich was then separated, and both the donor and acceptor compartments were assayed for the amount of material present, by comparison with the UV spectrum (225–500 nm) obtained from a pure reference standard. Mass balance was used to determine the amount of material remaining in the membrane barrier, with the molar amount lost to the membrane called %*R*.

Permeability (P_e) was calculated as described previously,[14,15] except that the filter area, 0.3 cm^2, was multiplied by the apparent porosity, 0.76. This latter step ensures that the UWL thickness determined from PAMPA assays using filters with a different porosity[21,52] would be on a comparable scale.

The buffers used in the assay are automatically prepared by the robotic system. The quality controls of the buffers are performed by alkalimetric titration, incorporating the Avdeef–Bucher procedure.[59] Following the completion of the UV assays, the pH in each microtitre plate well was measured to confirm correct value.

4.3.2. Permeability–pH profiles in PAMPA. For ionizable molecules, the pH-dependent membrane permeability,

P_m, is related to the pH-independent intrinsic permeability, P_0, as

$$P_m = f_u \cdot P_0 \quad (1)$$

where f_u is the fraction of the species in the uncharged form at a particular pH. For a weak base, B,

$$f_u = \frac{[B]}{[B]_{TOT}} = \frac{1}{(1 + 10^{pK_a - pH})} \quad (2)$$

A permeating molecule encounters two resistances in penetrating a PAMPA barrier, one due to the unstirred water layer adjacent to each side of the membrane barrier, and one due to the membrane itself. Since resistances are additive, and permeability is the inverse of resistance, the effective (measured) permeability, P_e, is related to the membrane and intrinsic permeability according to the relationship (weak base)

$$\frac{1}{P_e} = \frac{1}{P_u} + \frac{1}{P_m} = \frac{1}{P_u} + \frac{(1 + 10^{pK_a - pH})}{P_0} \quad (3)$$

where P_u is the unstirred water layer permeability. The two parameters, P_u and P_0, were solved by weighted regression analysis of Eq. 3 in the PAMPA Evolution software. In the procedure, it is necessary to know the value of the pK_a of the molecule.[60]

4.4. Molecular dynamics simulations

The conformational hypersurface of **1** and **2** was explored by Hybrid Monte Carlo (HMC) module implemented in MOE (see Section 4.6 for details). The HMC method accelerates the conventional MD search by periodically performing Monte Carlo steps across torsional energy barriers, thereby addressing the barrier crossing problem that is encountered in the standard MD algorithm.

Firstly three different geometries were randomly chosen as starting points on which HMC runs (iterations = 20,000; save period = 100; MD steps = 1, MD time step = 0.005 ps; temperature = 2000 K; equilibration steps = 100) were performed. The *S* enantiomers have always been considered according to X-ray data.[4] By adopted conditions 200 conformers for each starting structure were obtained, merged together and their geometries were optimized by MMFF94 force field.[61] The next step consisted in the RMS calculation which was performed using a PERL script. If their relative RMS was lower than 0.33, the conformers were considered equal and put in the same cluster. Finally, the lowest energy conformer of each cluster was included in the final databases which was sorted by increasing energy.

To investigate medium influences on conformation preferences the effect of solvation has also been tested in the minimization step by including the energy of solvation associated with the molecule being in a continuum solvent model; practically a set of electrostatic corrections are calculated with the GB/SA method[62] and applied to the MMFF94 force field as implemented in MOE. AM1 minimization on conformer of relevant interest was finally performed by incorporating (see Section 2) the Dixon/Hehre solvation model (water conditions).[63,64]

4.5. ASA descriptors

$FCASA^+$ descriptors have been calculated by MOE package (see below) on each conformer arising from molecular dynamics simulation, using PEOE charges, 1.4 Å as the radius probe.

$$FCASA^+ = \frac{CASA^+}{ASA} \quad (4)$$

where $FCASA^+$ is the fractional charge-weighted positive surface area, $CASA^+$ the charge-weighted positive surface area, and ASA the positive surface area.

$$CASA^+ = ASA^+ \cdot PC^+ \quad (5)$$

where PC^+ is the total positive partial charge.

4.6. Hardware and software

pK_a values have been calculated by ADME Boxes[19] and SPARC.[18]

Lipophilicity data were calculated by Absolv,[24] and by various algorithms (ALOGP, IAlogP, CLOGP, KOWWIN, XLOGP) available on-line at http://146.107.217.178/lab/alogps/.

Permeability predictions were by ADME Boxes.[19]

Molecular dynamics calculations were made by MOE (the molecular operating environment).[63]

The geometry optimizations performed with the AM1 semi-empirical methods were carried out with SPARTAN.[64]

All calculations described herein were performed on a Linux based biprocessor Appro 1124 server and on a standard IBM compatible computer.

Acknowledgements

G.C. and G.E. are indebted with Roberta Cavalli (University of Turin) for discussion and Sirius Analytical Instruments Ltd (Forest Row, UK) for donating the copy of Absolv software used for this research. We also thank the Institute of Medicinal Chemistry of the University of Lausanne (CH) for the use of Spartan.

References and notes

1. Reappraisal, A. *Drugs* **1998**, *55*, 509.
2. Epstein, M. *Drugs* **1999**, *57*, 1.
3. Herbette, L.; Vecchiarelli, M.; Leonardi, A. *J. Cardiovasc. Pharmacol.* **1997**, *29*, S19.

4. Arrowsmith, J. E.; Campbell, S. F.; Cross, P. E.; Stubbs, J. K.; Burges, R. A.; Gardiner, D. G.; Blackburn, K. J. *J. Med. Chem.* **1986**, *29*, 1696.
5. Alker, D.; Burges, R. A.; Campbell, S. F.; Carter, A. J.; Cross, P. E.; Gardiner, D. G.; Humphrey, M. J.; Stopher, D. A. *J. Chem. Soc., Perkin Trans. 2* **1992**, 1137.
6. Mason, P. R.; Campbell, S. F.; Wang, S.-D.; Herbette, L. *Mol. Pharmacol.* **1989**, *36*, 634.
7. Austin, R. P.; Davis, A. M.; Manners, C. N. *J. Pharm. Sci.* **1995**, *84*, 1180.
8. Caron, G.; Reymond, F.; Carrupt, P. A.; Girault, H. H.; Testa, B. *PSST* **1999**, *2*, 327.
9. Caron, G.; Ermondi, G.; Boschi, D.; Carrupt, P. A.; Fruttero, R.; Testa, B.; Gasco, A. *Helv. Chim. Acta* **1999**, *82*, 1630.
10. Caron, G.; Steyaert, G.; Pagliara, A.; Reymond, F.; Crivori, P.; Gaillard, P.; Carrupt, P. A.; Avdeef, A.; Comer, J. E.; Box, K. J.; Girault, H. H.; Testa, B. *Helv. Chim. Acta* **1999**, *82*, 1211.
11. Caron, G.; Gaillard, P.; Carrupt, P. A.; Testa, B. *Helv. Chim. Acta* **1997**, *80*, 449.
12. Dickins, M.; van de Waterbeemd, H. *Biosilico* **2004**, *2*, 38.
13. Avdeef, A. *Curr. Top. Med. Chem.* **2001**, *1*, 277.
14. Avdeef, A. High-throughput Measurements of Permeability Profiles. In *Drug Bioavailability. Estimation of Solubility, Permeability, Absorption and Bioavailability*, van de Waterbeemd, H., Lennernaes, H., Artursson, P., Eds.; Wiley-VCH: Weinheim, 2003; Vol. 3.
15. Avdeef, A. *Absorption and Drug Development. Solubility, Permeability, and Charge State*; New York: John Wiley & Sons, 2003; p 116.
16. Rolando, B.; Caron, G.; Marini, E.; Grosa, G.; Fruttero, R.; Gasco, A. *Med. Chem. Res.* **2003**, *11*, 322.
17. Franke, U.; Munk, A.; Wiese, M. *J. Pharm. Sci.* **1999**, *88*, 89.
18. SPARC Software, http://ibmlc2.chem.uga.edu/sparc/index.cfm, 2003.
19. ADME boxes Software, Version 1.6, Advanced Pharma Algorithms, 2003.
20. Testa, B.; Crivori, P.; Reist, M.; Carrupt, P. A. *The Influence of Lipophilicity on the Pharmacokinetic Behavior of Drugs: Concepts and Examples*; Kluwer Academic, 2000; p 179.
21. Faller, B.; Wohnsland, F. Physicochemical Parameters as Tools in Drug Discovery and Lead Optimisation. In *Pharmacokinetic Optimization in Drug Research*, Testa, B., van de Waterbeemd, H., Folkers, G., Guy, R. H., Eds.; Wiley-VCH: Zürich, 2001; Vol. 1, p 257.
22. Caron, G.; Ermondi, G. *Mini Rev. Med. Chem.* **2003**, *3*, 821.
23. Lombardo, F.; Shalaeva, M. Y.; Tupper, K. A.; Gao, F.; Abraham, M. H. *J. Med. Chem.* **2000**, *43*, 2922.
24. Absolv Software, Version 1.0, Forrest Row, UK, Sirius Analytical Instruments Ltd, 2000.
25. Avdeef, A.; Testa, B. *CMLS* **2002**, *59*, 1681.
26. Steyaert, G.; Lisa, G.; Gaillard, P.; Boss, G.; Reymond, F.; Girault, H. H.; Carrupt, P. A.; Testa, B. *J. Chem. Soc., Faraday Trans.* **1997**, *93*, 401.
27. Galland, A.; Bouchard, G.; Caron, G.; Plemper van Balen, G.; a Marca Martinet, C.; Geinoz, S.; Rey, S.; Ermondi, G.; Vacondio, F.; Mor, M.; Plazzi, P. V.; Carrupt, P. A.; Testa, B. *Chimia* **2002**, *56*, 373.
28. Pagliara, A.; Caron, G.; Lisa, G.; Fan, W.; Gaillard, P.; Carrupt, P. A.; Testa, B.; Abraham, M. H. *J. Chem. Soc., Perkin Trans. 2* **1997**, 2639.
29. Bouchard, G.; Carrupt, P. A.; Testa, B.; Gobry, V.; Girault, H. H. *Chem. Eur. J.* **2002**, *8*, 3478.
30. Plempler van Balen, G.; a Marca Martinet, C.; Caron, G.; Bouchard, G.; Reist, M.; Carrupt, P. A.; Fruttero, R.; Gasco, A.; Testa, B. *Med. Res. Rev.* **2003**, *24*, 299.
31. Bäuerle, H.-D.; Seelig, J. *Biochemistry* **1991**, *30*, 7203.
32. Herbette, L.; Rhodes, D. G.; Preston Mason, R. *Drug Des. Delivery* **1991**, *7*, 75.
33. Preston Mason, R. *Biochem. Pharmacol.* **1993**, *45*, 2173.
34. Barbato, F.; LaRotonda, M. I.; Quaglia, F. *Eur. J. Med. Chem.* **1996**, *31*, 311.
35. Lombardo, F.; Shalaeva, M. Y.; Tupper, K. A.; Gao, F. *J. Med. Chem.* **2001**, *44*, 2490.
36. Goldmann, S.; Stoltefuss, J. *Angew. Chem., Int. Ed. Engl.* **1991**, *30*, 1559.
37. Cotta Ramusino, M.; Vari, M. R. *J. Mol. Struct. Theochem.* **1999**, *492*, 257.
38. Cruciani, G.; Crivori, P.; Carrupt, P. A.; Testa, B. *J. Mol. Struct. Theochem.* **2000**, *503*, 17.
39. Gaillard, P.; Carrupt, P. A.; Testa, B.; Boudon, A. *J. Comput.-Aided Mol. Des.* **1994**, *8*, 83.
40. Rey, S.; Caron, G.; Ermondi, G.; Gaillard, P.; Pagliara, A.; Carrupt, P. A.; Testa, B. *J. Mol. Graphics* **2001**, *19*, 521.
41. Stanton, D. T.; Jurs, P. C. *Anal. Chem.* **1990**, *62*, 2323.
42. Caron, G.; Ermondi, G. New Insights Into the Lipophilicity of Ionized Species. In *Physicochemical and Biological Profiling in Drug Research*, Testa, B., van de Waterbeemd, H., Folkers, G., Guy, R. H., Eds.; Wiley-VCH: Zürich, in press.
43. Kansy, M.; Senner, F.; Gubernator, K. *J. Med. Chem.* **1998**, *41*, 1007.
44. Murdock, D.; Heel, R. C. *Drugs* **1991**, *41*, 478.
45. Avdeef, A. High-Throughput Solubility and Permeability: MAD from G2-PAMPA. In *Physicochemical and Biological Profiling in Drug Research*, Testa, B., van de Waterbeemd, H., Folkers, G., Guy, R. H., Eds.; Wiley-VCH: Zürich, in press.
46. Alker, D.; Campbell, S. F.; Cross, P. E.; Burges, R. A.; Carter, A. J.; Gardiner, D. G. *J. Med. Chem.* **1990**, *33*, 585.
47. Avdeef, A.; Box, K. J.; Comer, J. E.; Gilges, M.; Hadley, M.; Hibbert, C.; Patterson, W.; Tam, K. Y. *J. Pharm. Biomed. Anal.* **1999**, *20*, 631.
48. Avdeef, A.; Comer, J. E. A.; Thomson, S. J. *Anal. Chem.* **1993**, *65*, 42.
49. Kansy, M.; Fischer, H.; Kratzat, K.; Senner, F.; Wagner, B.; Parrilla, I. High-throughput Artificial Membrane Permeability Studies in Early Lead Discovery and Development. In *Pharmacokinetic Optimization in Drug Research*, Testa, B., van de Waterbeemd, H., Folkers, G., Guy, R. H., Eds.; Wiley-VCH: Zürich, 2001; Vol. 1, p 447.
50. Avdeef, A.; Strafford, M.; Block, E.; Balogh, M. P.; Chambliss, W.; Khan, I. *Eur. J. Pharm. Sci.* **2001**, *14*, 271.
51. Avdeef, A. High-throughput Measurements of Solubility Profiles. In *Pharmacokinetic Optimization in Drug Research*; Testa, B., van de Waterbeemd, H., Folkers, G., Guy, R. H., Eds.; Wiley-VCH: Zürich, 2001; Vol. 1, p 305.
52. Wohnsland, F.; Faller, B. *J. Med. Chem.* **2001**, *44*, 923.
53. Sugano, K.; Hamada, H.; Machida, M.; Ushio, H.; Saitoh, K.; Terada, K. *Int. J. Pharm.* **2001**, *228*, 181.
54. Sugano, K.; Hamada, H.; Machida, M.; Ushio, H. *J. Biomol. Screen.* **2001**, *6*, 189.
55. Sugano, K.; Takata, N.; Machida, M.; Saitoh, K.; Terada, K. *Int. J. Pharm.* **2002**, *241*, 241.
56. Zhu, C.; Jiang, L.; Chen, T.-M.; Hwang, K.-K. *Eur. J. Med. Chem.* **2002**, *37*, 399.

57. Veber, D. F.; Johnson, S. R.; Cheng, H. Y.; Smith, B. R.; Ward, K. W.; Kopple, K. D. *J. Med. Chem.* **2002**, *45*, 2615.
58. Lennernaes, H. *J. Pharm. Sci.* **1998**, *87*, 403.
59. Avdeef, A.; Bucher, J. J. *Anal. Chem.* **1978**, *50*, 2137.
60. Walter, A.; Gutknecht, J. *J. Membr. Biol.* **1984**, *77*, 255.
61. Halgren, T. A. *J. Comput. Chem.* **1999**, *20*, 720.
62. Qiu, D.; Shenkin, P. S.; Hollinger, F. P.; Still, W. C. *J. Phys. Chem. A* **1997**, *101*, 3005.
63. MOE Software, Version 02, Montreal, Quebec Canada, Chemical Computing Group, Inc. 2003.
64. Spartan Software, Version 4.1. Irvine, California, Wavefunction, Inc. 1995.